

MICROCOPY RESOLUTION TEST CHART
NATIONAL BUREAU OF STANDARDS-1963-A

12

ADA 123 403

MARTIN MARIETTA

Martin Marietta
Laboratories

MML TR-23(c)

MECHANICAL PROPERTIES OF ADHESIVELY
BONDED ALUMINUM STRUCTURES PROTECTED
WITH HYDRATION INHIBITORS

End-of-Second-Year Report

November 1982

Unclassified

DTIC
JAN 14 1983
H

Prepared for:

Department of the Navy
Office of Naval Research
Arlington, Virginia 22217

Prepared by:

Martin Marietta Laboratories
1450 South Rolling Road
Baltimore, Maryland 21227-3898

Under
ONR Contract N00014-80-C-0718

DISTRIBUTION STATEMENT A
Approved for public release
Distribution Unlimited

05 01 14 010

SECURITY CLASSIFICATION OF THIS PAGE (When Data Entered)

REPORT DOCUMENTATION PAGE		READ INSTRUCTIONS BEFORE COMPLETING FORM
1. REPORT NUMBER	2. GOVT ACCESSION NO. AD - A123403	3. RECIPIENT'S CATALOG NUMBER
4. TITLE (and Subtitle) "Mechanical Properties of Adhesively Bonded Aluminum Structures Protected with Hydration Inhibitors"		5. TYPE OF REPORT & PERIOD COVERED End-of-Second-Year Report
		6. PERFORMING ORG. REPORT NUMBER MML TR-23(c)
7. AUTHOR(s) D.A. Hardwick, J.S. Ahearn, and J.D. Venables		8. CONTRACT OR GRANT NUMBER(s) N00014-80-C-0718
9. PERFORMING ORGANIZATION NAME AND ADDRESS Martin Marietta Laboratories 1450 South Rolling Road Baltimore, Maryland 21227		10. PROGRAM ELEMENT, PROJECT, TASK AREA & WORK UNIT NUMBERS
11. CONTROLLING OFFICE NAME AND ADDRESS Department of the Navy Office Of Naval Research Arlington, Virginia 22217		12. REPORT DATE November 1982
		13. NUMBER OF PAGES 34
14. MONITORING AGENCY NAME & ADDRESS (if different from Controlling Office) Baltimore DCAS Management Area 300 East Joppa Road, Room 200 Towson, Maryland 21204		15. SECURITY CLASS. (of this report) Unclassified
		15a. DECLASSIFICATION/DOWNGRADING SCHEDULE
16. DISTRIBUTION STATEMENT (of this Report) Unlimited distribution.		
17. DISTRIBUTION STATEMENT (of abstract entered in Block 20, if different from Report)		
18. SUPPLEMENTARY NOTES		
19. KEY WORDS (Continue on reverse side if necessary and identify by block number) Adhesive bonding, mechanical properties, organic inhibitors, bond durability, FPL, PAA.		
20. ABSTRACT (Continue on reverse side if necessary and identify by block number) Our research has shown that an adsorbed monolayer of the organic inhibitor nitrilotris (methylene) phosphonic acid (NTMP) improves the bond durability of 2024 Al adherends prepared by phosphoric acid anodization (PAA). As had previously been determined for Forest Products Laboratories (FPL)-prepared adherends, maximum improvements in bond durability occurred when a monolayer of NTMP was adsorbed onto the surface. Examination of the wedge test failure surfaces of PAA adherends treated in NTMP revealed that although crack propagation had initially involved oxide-to-hydroxide conversion of the original PAA oxide, the		

locus of failure transfers to the adhesive near the interface quite early in the test. This means that the failure of NTMP-treated PAA adherends was predominantly cohesive through the adhesive. In addition, the presence of NTMP at the oxide/adhesive interface did not degrade the initial bond strength when epoxy-based adhesive systems were used.

This hydration inhibitor scheme shows considerable promise for improving the durability of adhesively-bonded components for military and commercial aircraft. The process has the advantage of being extremely simple; aluminum surfaces prepared for adhesive bonding need only be dipped or sprayed with a very dilute (~ 100-ppm) aqueous solution of the organic inhibitor. The very thin inhibitor layer does not interfere with interlocking between the microscopically-rough oxide and the adhesive, which is the source of the high bond strength essential to aircraft applications.

Accession No.	
NTIS or DTIC ID	<input checked="" type="checkbox"/>
Unannounced Justification	<input type="checkbox"/>
By _____	
Distribution _____	
Availability _____	
Dist _____	
A	



MML TR-23(c)

MECHANICAL PROPERTIES OF ADHESIVELY BONDED ALUMINUM
STRUCTURES PROTECTED WITH HYDRATION INHIBITORS

End-of-Second-Year Report on
ONR Contract N00014-80-C-0718


November 1982

Prepared for:

Department of the Navy
Office of Naval Research
Arlington, Virginia 22217

Prepared by:

D. A. Hardwick, J. S. Ahearn, and J. D. Venables
Martin Marietta Laboratories
1450 South Rolling Road
Baltimore, Maryland 21227



J. S. Ahearn
Principal Investigator

TABLE OF CONTENTS

	<u>Page</u>
1. INTRODUCTION	1
2. EXPERIMENTAL METHOD	
2.1 SURFACE PREPARATION	6
2.2 WEDGE-TEST PROCEDURE	6
2.3 T-PEEL PROCEDURE	8
2.4 SURFACE ANALYSIS AND EXAMINATION	9
3. RESULTS	
3.1 INHIBITOR SURFACE COVERAGE	11
3.2 T-PEEL TESTS	11
3.3 WEDGE TESTS	12
3.4 SURFACE EXAMINATION OF WEDGE-TEST FAILURE SURFACES	16
3.5 SURFACE ANALYSIS OF WEDGE-TEST FAILURE SURFACES	24
4. DISCUSSION	28
5. REFERENCES	34

LIST OF FIGURES

<u>No.</u>		<u>Page</u>
1	Stereo micrograph of Al-oxide morphology on FPL adherends and schematic of oxide structure. ⁽¹⁾	2
2	Stereo micrograph of Al-oxide morphology on PAA adherends and schematic of oxide structure. ⁽¹⁾	3
3	Crack length vs time for FPL and PAA adherends and PAA adherends treated with 10- and 300-ppm NTMP solution.	13
4	Crack length vs time for PAA adherends and PAA treated in 10-ppm NTMP solution at either room temperature or 80°C.	14
5	Crack length vs time for PAA adherends and PAA treated in 300-ppm NTMP solution at either room temperature or 80°C.	15
6	Crack length vs time for PAA adherends and PAA treated in 10-, 100-, or 500-ppm NTMP solution.	17
7	Average crack velocity, v , as a function of G , the fracture energy.	18
8	SEM micrograph of "dull" region on Al side of wedge test failure surface. Adherend was PAA-treated in 100-ppm NTMP solution.	21
9	SEM micrographs of: (a) transition region on Al side of PAA wedge-test failure surface [arrow denotes direction of crack propagation]; (b) transition region at higher magnification; (c) failure through near-surface adhesive layer.	22
10	SEM micrographs of Al side of failure surface on PAA adherend treated in 200-ppm NTMP solution showing hydroxide formation after crack propagation through the adhesive layer.	23
11	Depth profile of "dull" region on Al side of PAA wedge-test failure surface.	26
12	Depth profile of "shiny" region on Al side of PAA wedge-test failure surface.	27

LIST OF TABLES

<u>No.</u>	<u>Title</u>	<u>Page</u>
1	Surface Coverage (P/Al Ratio Determined by XPS), as a Function of NTMP Concentration and Temperature, on PAA-Prepared Al Surfaces.	11
2	Surface Composition (at %) of Al Side of Wedge-Test Failures as Determined by XPS.	24

1. INTRODUCTION

Two important factors that determine the overall performance and success of adhesively bonded aluminum structures are the initial bond strength of the adherend/adhesive interface and the stability of the interface in a humid environment. Recent studies at Martin Marietta Laboratories⁽¹⁾ have indicated that the initial bond strength of commercial aerospace bonding processes is determined principally by physical interlocking between the oxide on the Al adherend and the adhesive.

The Al-oxide morphologies of two commercial processes are illustrated in Figs. 1 and 2. The Forest Products Laboratory process (FPL) produces an oxide morphology consisting of oxide cells roughly 400 Å in diameter and whisker-like structures 400 Å high (Fig. 1). The phosphoric acid anodization process (PAA) also produces an oxide morphology consisting of oxide cells and whiskers (Fig. 2), but the cells are much higher (~ 3,000 Å) than those produced by FPL. In both cases, the rough oxide surface interlocks with the overlaying adhesive to form a much stronger bond than would be possible with a smooth oxide surface.

The long-term durability of the Al-oxide adhesive bond is determined to some extent by physical interlocking, but recent evidence from our research⁽²⁾ indicates that bond durability is also controlled by conversion of the original adherend oxide to a hydroxide in the presence of moisture. A distinction must be drawn when comparing bond durability observed with a smooth adherend oxide morphology and the durability of a rough one. For adherends with smooth morphology, the bond strength

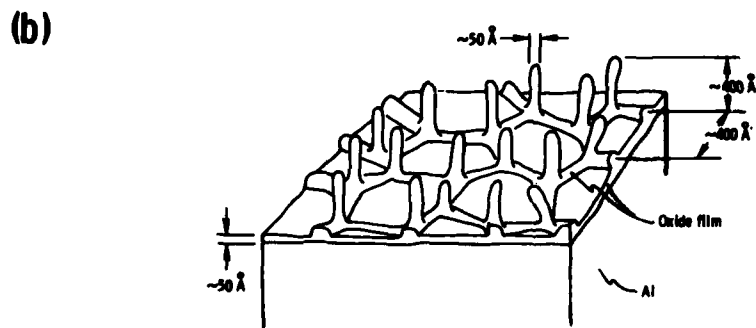
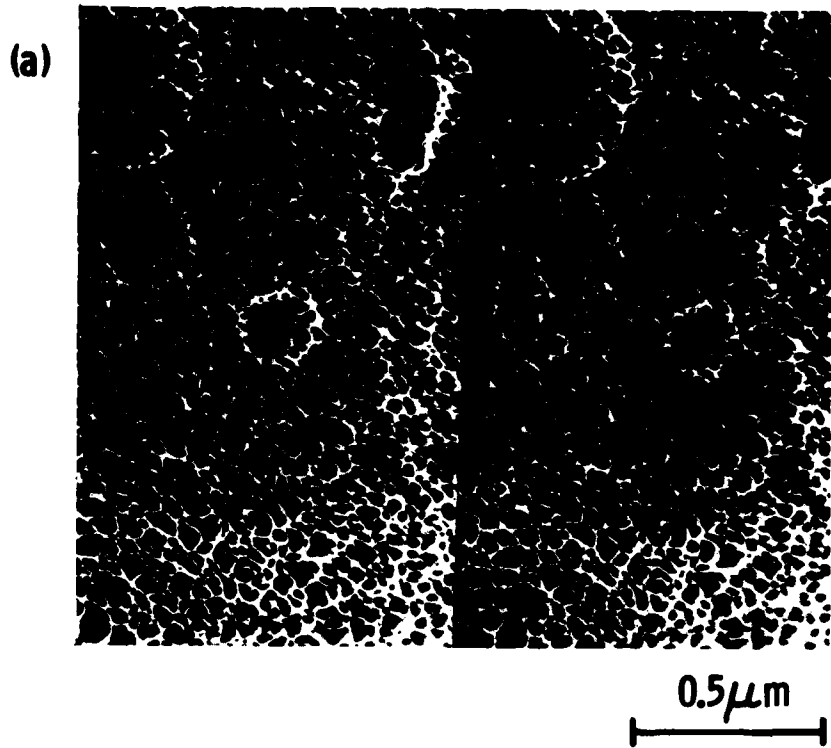


Figure 1. Stereo micrograph of Al oxide morphology on FPL adherends and schematic of oxide structure (1).

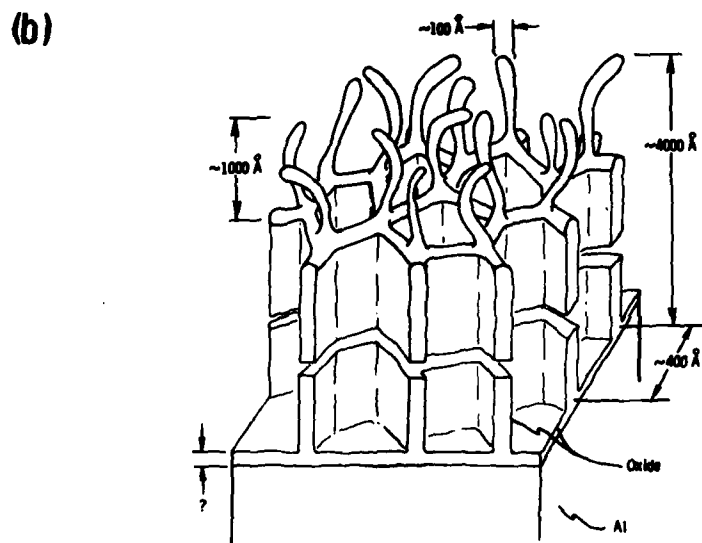
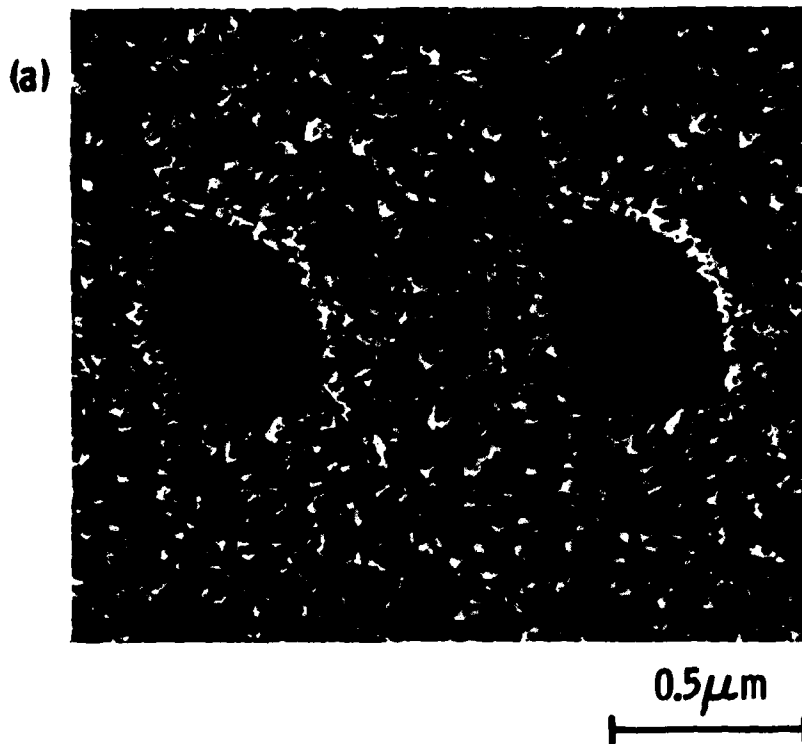


Figure 2. Stereo micrograph of Al oxide morphology on PAA adherends and schematic of oxide structure (1).

depends on the chemical interaction between the Al-oxide surface and adhesive molecules. Water penetration to a crack tip can disrupt the chemical bonds between Al-oxide and polymer molecules and cause relatively rapid crack propagation. For adherends with rough oxide morphology, the breaking of chemical bonds by water does not affect crack propagation because physical interlocking of the adhesive and oxide prevents it. Crack movement is only possible if the interlocking of adhesive and oxide is somehow destroyed. Our recent work⁽²⁾, indicates that the conversion of the Al-oxide to Al-hydroxide disrupts the interlocking and degrades the bond.

These results led us to consider methods that would serve to inhibit the oxide-to-hydroxide conversion process and thereby improve the long-term durability of adhesively bonded aluminum structures. In particular, we have been investigating the use of certain organic acids (amino phosphonates), which, when adsorbed in monomolecular form on the oxide, drastically retard the rate of the conversion process without interfering with the mechanical interlocking that is so important for obtaining good initial bond strength.

In the first year report under this program (ONR N00014-80-C-0718), we concluded⁽³⁾ that hydration inhibitors, and particularly nitrilotris (methylene) phosphonic acid (NTMP), can be used to improve the bond durability of adherends etched in FPL. In fact, the presence of NTMP improves the durability of FPL-prepared 2024 Al adherends to the point where they rival the durability of PAA adherends. Analysis of the results suggested that an inhibitor's effectiveness depends both on its ability

to inhibit the conversion of Al-oxide to hydroxide and to form chemical bonds with the adhesive.

In the continuation of this program, we have extended the use of the inhibitor NTMP to PAA-prepared adherends. We have also investigated the compatibility of the NTMP inhibitor, as adsorbed on an adherend oxide surface, with several primer/adhesive systems that are widely used in structural bonding applications.

2. EXPERIMENTAL METHOD

2.1 SURFACE PREPARATION

The initial step in the preparation of test coupons and panels was degreasing; panels were immersed for 15 minutes in an agitated solution of Turco 4215* (44 g/l) at 65°C and then rinsed in distilled, deionized water. Degreasing was followed by a standard FPL treatment, consisting of a 15-minute immersion in an agitated aqueous solution of sodium dichromate dihydrate (60 g/l) and sulfuric acid (17% v/v) held at 65°C, after which samples were rinsed in distilled, deionized water and air dried. FPL-treated panels were then treated using the PAA process. Panels were anodized in a 10 wt % phosphoric acid solution at a potential of 10 V for 20 minutes, followed by a rinse in distilled, deionized water and air drying.

The treatment of panels in inhibitor solutions after the PAA process was accomplished by immersing the panels for 30 minutes in an aqueous solution of the inhibitor held at either room temperature or 80°C, followed by rinsing in distilled, deionized water and air drying. The inhibitor used was nitrilotris (methylene) phosphonic acid (NIMP): $N[CH_2P(O)(OH)_2]_3$.

2.2 WEDGE TEST PROCEDURE

Following surface preparation, 2024 Al adherends (6 x 6 x 0.125 in.) were bonded together using American Cyanamid FM 123-2 adhesive cured at 120°C and 40 psi for 1 hour. The bonded panels were cut into 1 x 6 in. test strips and a wedge (0.125 in. thick) was inserted between

* An alkaline cleaning agent manufactured by Turco Products.

the two adherends to provide a stress at the bondline. After an equilibration period of 1 hour at ambient conditions, the wedge-test samples were placed in a humidity chamber held at 60°C and 98% relative humidity. In order to determine the extent of crack propagation, the test pieces were periodically removed from the humidity chamber and examined under an optical microscope to locate and mark the position of the crack front. When the test was complete, usually after 150 to 160 hours, calipers were used to measure the positions of these marks, which denote crack length as a function of time.

Wedge-test specimens are the adhesive-joint analogue of the wedge-force loaded double-cantilever beam (DCB) specimens used in the testing of homogeneous materials. In a wedge-loaded DCB, the displacement is necessarily fixed, and the load decreases during crack growth. If the crack length, a , is measured from the point of load application, then it follows from simple beam theory that the load can be expressed as a function of the fixed displacement, w , as:⁽⁴⁾

$$P = \frac{Bh^3Ew}{8a^3} \quad (1)$$

where: P = load at point of application
 E = Young's modulus of adherends
 h = thickness of adherends
 B = width of adherends
 w = thickness of wedge
 a = crack length

If the crack is not growing, then the load is proportional to the displacement: $P = w/C$. C is the compliance (i.e., inverse of the stiffness) of the adherends. Thus, from the above relation:

$$C = \frac{w}{P} = \frac{8a^3}{Eh^3B} \quad (2)$$

Using the Griffith energy criterion, G , the "energy release rate" or "crack extension force" is given by:

$$G = \frac{P^2}{2B} \frac{\partial C}{\partial a} \quad (3)$$

$$\text{i.e., } G = \frac{3h^3Ew^2}{16a^4} \quad (4)$$

Equation (4) shows that the crack extension force decreases with the fourth power of the crack size. This equation can be modified to take into account such factors as ductile strain in the adhesive, which would allow rotation of the adherends ahead of the crack tip.⁽⁵⁾ As the test was used for comparison, and the same adhesive was always employed, these corrections were not used in the analysis of the wedge-test data.

Using the crack-length data generated by the wedge tests, the crack extension force, G , was calculated using Eq. (4). The average crack velocity, v , was also determined from the information on crack length as a function of time.

2.3 T-PEEL PROCEDURE

The material used for T-peel testing was 2024 Al clad with a 1000 series Al alloy. Prepared panels, 6 x 12 x 0.032 in., were bonded together over approximately 9 in. of their length using one of the primer/adhesive systems listed below.

<u>Primer/Adhesive System</u>	<u>Cure Conditions</u>
1. No primer FM 123-2 adhesive	60 min at 120°C (250°F) and 40 psi
2. BR 127 primer FM 300M adhesive	30 min at RT + 60 min at 120°C (250°F) 60-90 min at 175°C (350°F) and 45 psi
3. No primer FM 53 adhesive	60 min at 120°C (250°F) at 45 psi.

The bonded panels were then cut into 1 in.-wide test specimens. The 3 in.-long unbonded ends were bent apart, perpendicular to the glue line, and clamped into the grips of an Instron tensile-testing machine. Testing was done at a constant cross-head speed of 10 in./min, and a record was made of load versus cross-head movement.

2.4 SURFACE ANALYSIS AND EXAMINATION

On completion of the wedge and T-peel tests, the bonded pairs were separated and samples were selected for surface analysis and examination in the scanning transmission electron microscope (STEM). The surface analysis measurements were done with a Physical Electronics spectrometer (Model 548) equipped with a double-pass cylindrical mirror analyzer. Measurements were taken in both the XPS (X-ray photoelectron spectroscopy) and AES (Auger electron spectroscopy) modes, the latter being used in conjunction with sputter-etching (argon ions) to obtain information on composition as a function of depth.

Crack surfaces were examined in a JEOL-100 CX scanning transmission electron microscope (STEM) used in the high-resolution (20 ~ 30 Å) SEM mode. To suppress charging of the surface by the electron beam, a thin coating of Pt was deposited on the surfaces by secondary ion deposition.

Test coupons were analyzed using XPS to determine the amount of inhibitor adsorbed on the oxide surface. The peak height of the 2p photoelectrons of P and Al was measured and the P/Al ratio was calculated using previously determined sensitivity factors.⁽⁶⁾ The P/Al ratio was taken as a measure of the relative coverage of inhibitor on the Al-oxide surface.

3. RESULTS

3.1 INHIBITOR SURFACE COVERAGE

The inhibitor surface coverage on PAA oxide surfaces, as given by the P/Al ratio, is summarized in Table 1. Only a limited amount of data was collected, but the range of solution concentrations used was similar to that used to evaluate inhibitor adsorption on FPL.(3)

TABLE 1

Surface Coverage (P/Al Ratio Determined By XPS), As a Function Of NTMP Concentration And Temperature, On PAA Prepared Al Surfaces

NTMP concentration (ppm)	Solution Temperature	Surface Coverage (P/Al)
0	RT	0.11 ± 0.03
1	RT	0.13 ± 0.01
10	RT	0.16 ± 0.01
300	RT	0.20 ± 0.05
300	80°C	0.49 ± 0.04

3.2 T-PEEL TESTS

For each adhesive system tested, T-peel specimens were prepared using the following surface treatments: 1) FPL, 2) FPL + 10-ppm NTMP (RT), 3) FPL + 100-ppm NTMP (RT), and sometimes 4) FPL + 300-ppm NTMP (80°C).

In the course of investigating adhesive systems of varying T-peel strengths, three epoxy-based adhesives or adhesive/primer combinations were investigated; they are listed below with their experimentally determined T-peel strengths.

<u>Primer/Adhesive</u>	<u>T-peel Strength (lb/in)</u>	
BR 127/FM 300M	6.0	1.0
- /FM 123-2	15.0 ± 0.9	
- /FM 53	50.9 ± 5.7	

In each case, the T-peel strength values were not influenced by the presence of NTMP at the oxide/epoxy interface since failure occurred cohesively through the adhesive. Each of the values obtained was comparable with the strength claimed by the manufacturer for the adhesive under the test conditions employed here.

3.3 WEDGE TESTS

The wedge test results (Fig. 3) for FPL adherends, PAA adherends, and PAA adherends treated with low (10-ppm) and high (300-ppm) concentration NTMP solutions demonstrate the superior bond durability of PAA-treated adherends compared with FPL-treated adherends and also show that durability can be further improved by pretreatment with NTMP. As shown in Fig. 3, treating the surface in a 300-ppm NTMP solution gave little further improvement, as gauged by final crack length, over treatment in a 10 ppm solution. This probably results from the similar surface coverages obtained by treatment in 10- and 300-ppm solutions.

In Figs. 4 and 5, wedge test results have been plotted for two concentrations of NTMP solution, 100 ppm and 300 ppm respectively, at two temperatures, RT and 80°C (176°F). Treatment in the elevated temperature 10-ppm NTMP solution gave no improvement over the 10-ppm solution used at room temperature (Fig. 4). When adherends were treated in a high concentration solution (300 ppm) at 80°C, there actually appeared to be a decrease in bond durability in comparison with adherends treated in 300-ppm NTMP solution at room temperature (Fig. 5).

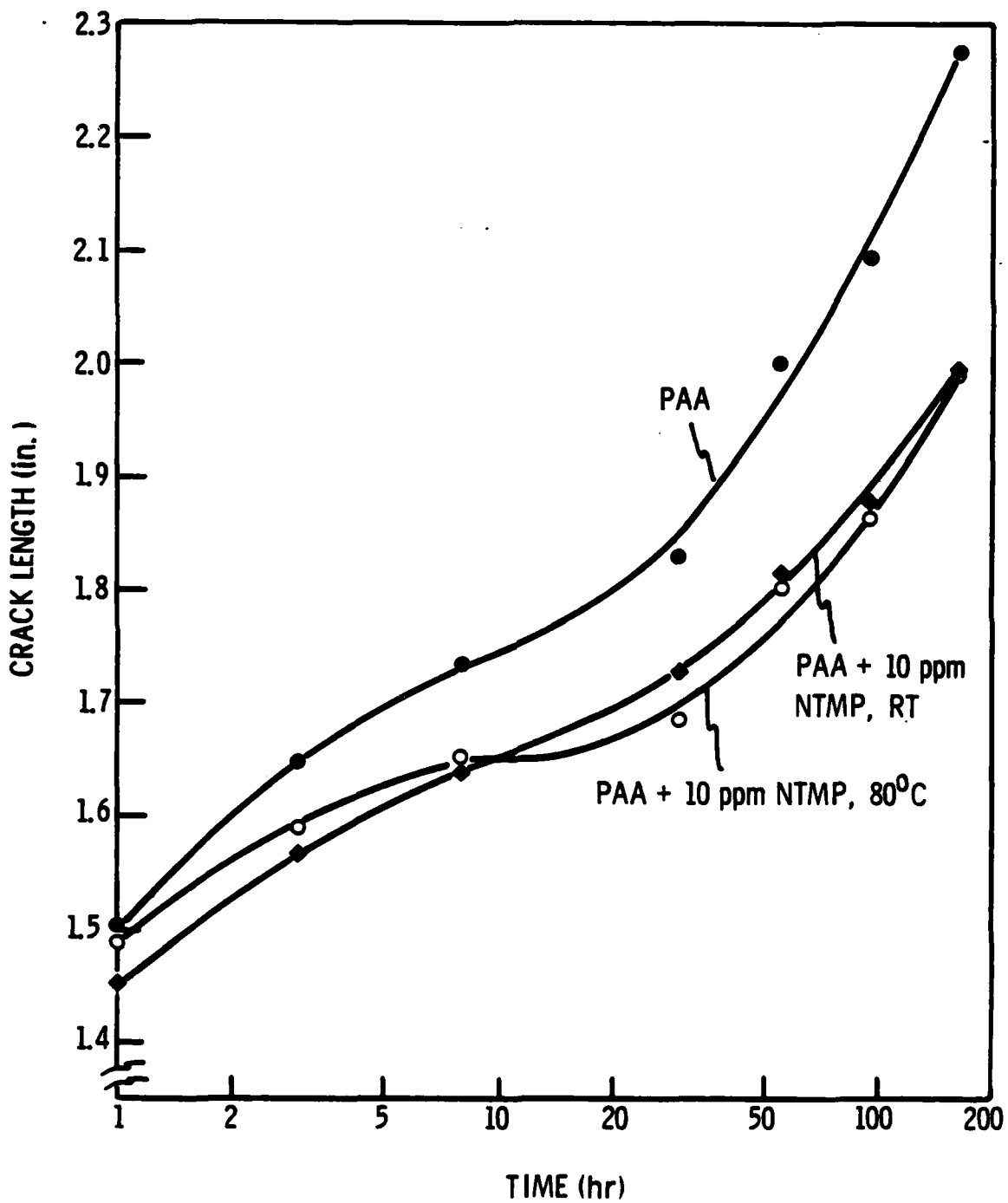


Figure 4. Crack length vs time for PAA adherends and PAA treated in 10-ppm NTMP solution at either room temperature or 80°C.

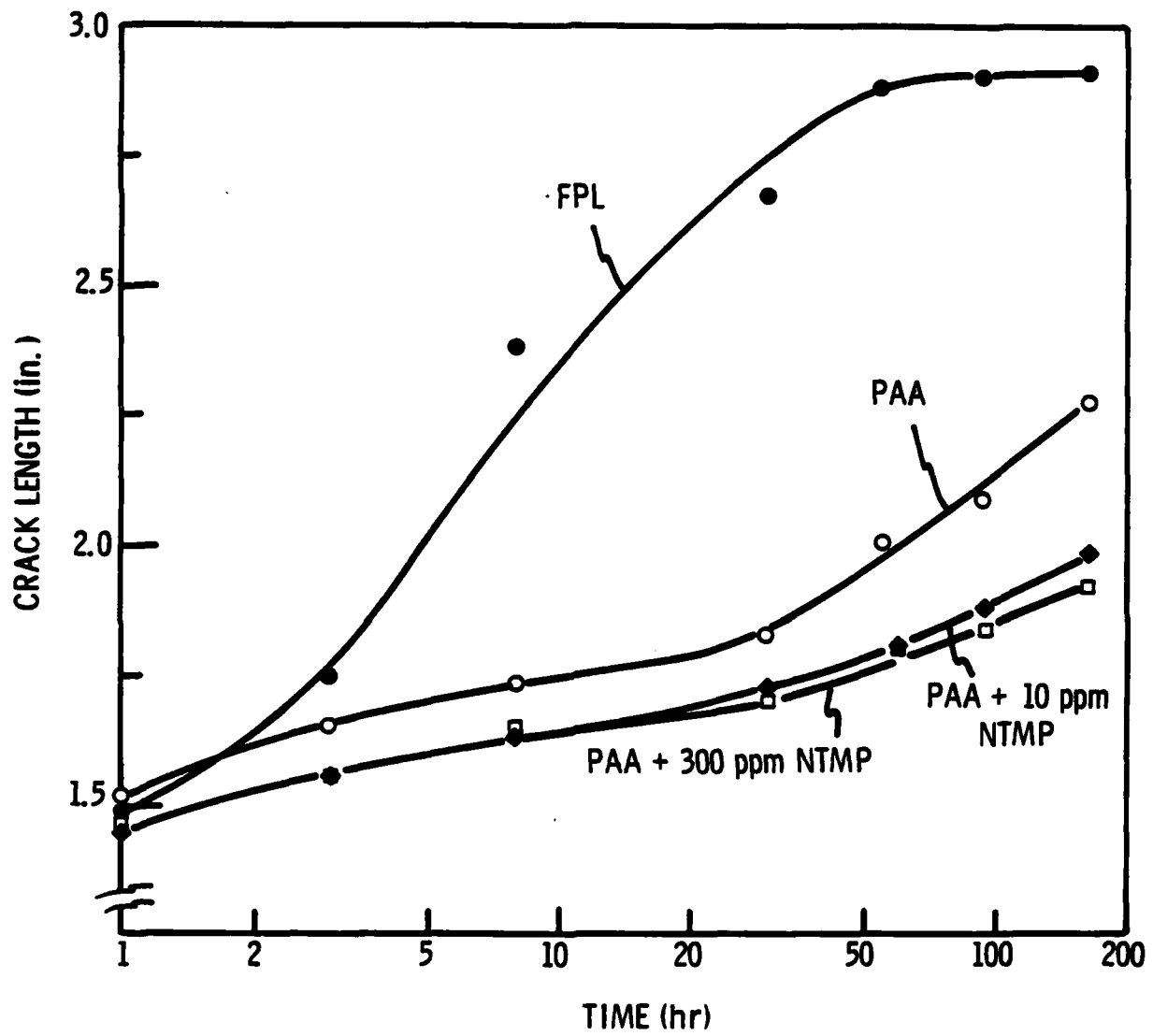


Figure 3. Crack length vs time for FPL and PAA adherends and PAA adherends treated with 10-ppm and 300-ppm NTMP solution.

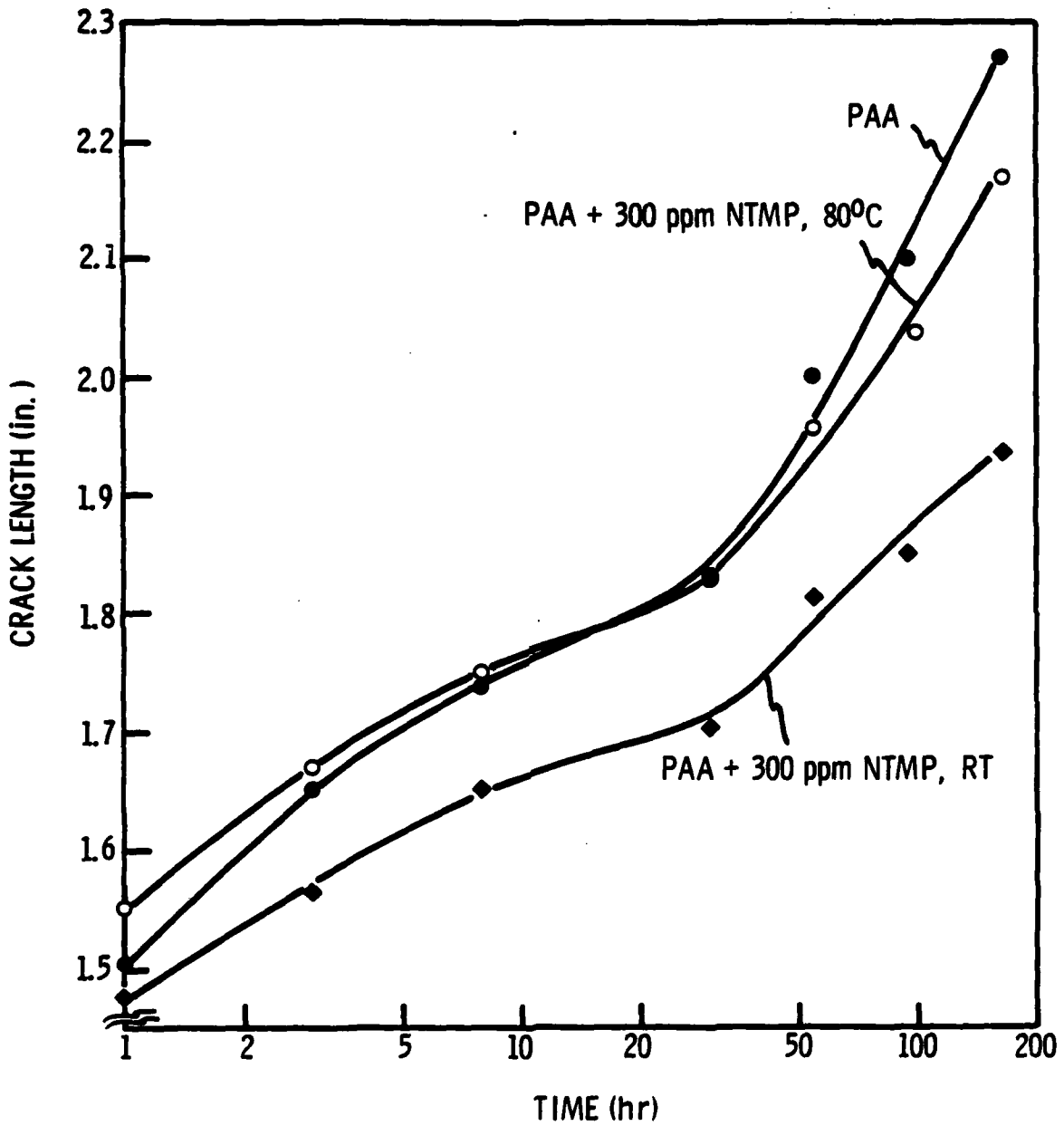


Figure 5. Crack length vs time for PAA adherends and PAA treated in 300-ppm NTMP solution at either room temperature or 80°C.

In a further series of wedge tests (Fig. 6) the 10 ppm NTMP treated adherends did not behave as well as in the previous test. Surface coverage results for NTMP on FPL-treated surfaces indicated⁽³⁾ some variability in the adsorption of NTMP on Al-oxide, particularly when the solution concentration is below the level necessary to establish monolayer coverage. Such scatter in surface coverage at the 10-ppm NTMP level probably causes the variability in wedge-test performance for samples treated in these solutions. However, once monolayer coverage is established on the surface (thought to be with $P/Al \sim 0.15-0.20$) the results are highly reproducible. In addition to the results for adherends treated in 100-ppm and 500-ppm NTMP solutions (reported in Fig. 6), tests were also conducted using PAA adherends treated in 200-ppm and 300-ppm NTMP solutions. The behavior of these adherends was the same as the behavior of the 100-ppm and 500-ppm NTMP treated adherends (within experimental scatter), indicating that monolayer coverage of NTMP achieves, optimal performance.

As outlined in the experimental procedure (Section 2.2) the wedge test results were analyzed to yield crack extension forces and resultant crack velocities. The results of this data analysis (discussed below) are shown in Fig. 7. As G decreases over the duration of the test, the initial G values are those on the right-hand side of the graph. The three curves represent data from wedge tests of FPL and PAA adherends and PAA adherends treated with 100-500 ppm NTMP.

3.4 SURFACE EXAMINATION OF WEDGE TEST FAILURE SURFACE

Visual Examination

At the conclusion of the humidity exposure, the wedge test assemblies were broken open. The crack propagation region, delineated by the

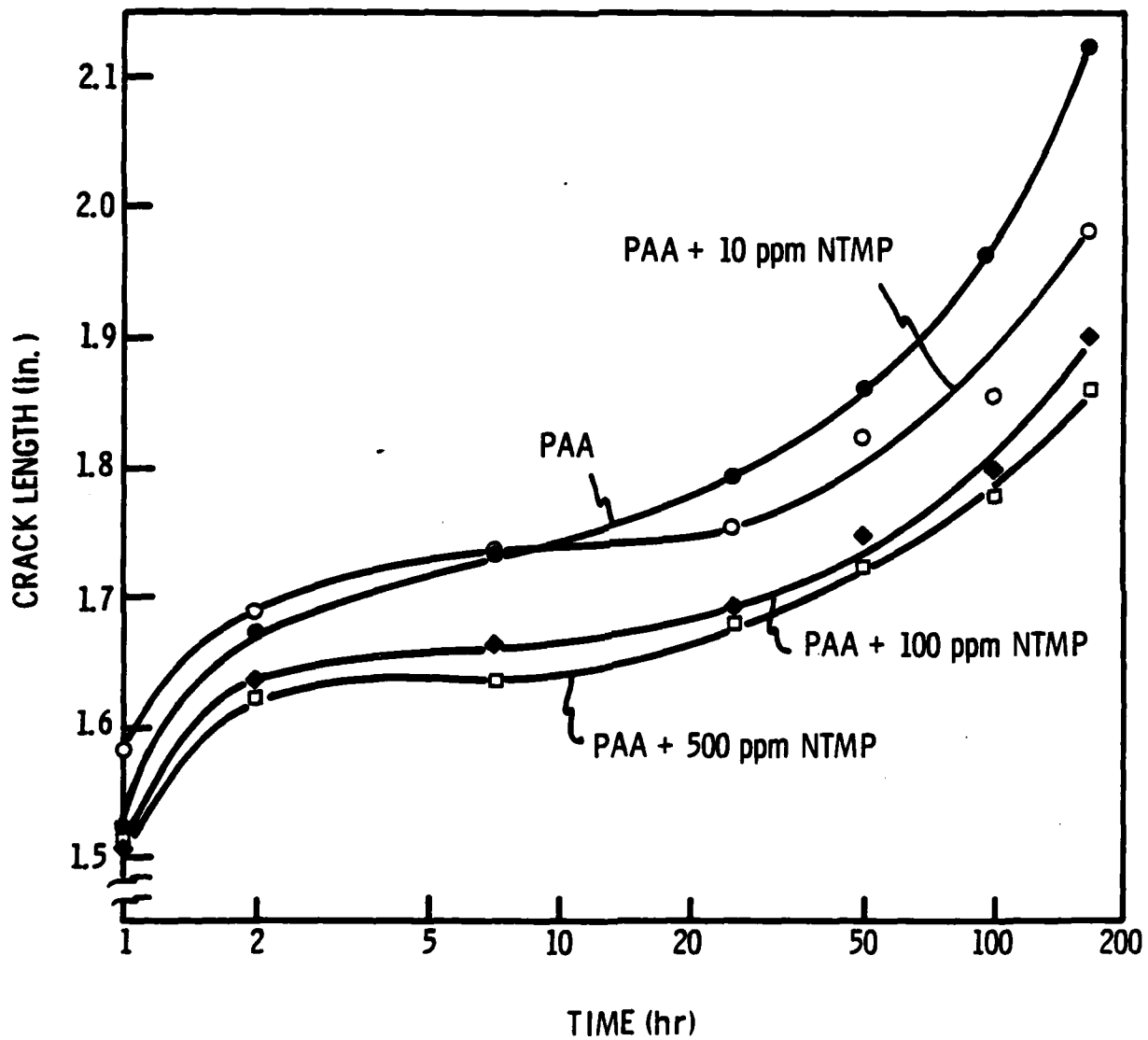


Figure 6. Crack length vs time for PAA adherends and PAA treated in 10-ppm, 100-ppm or 500-ppm NTMP solution.

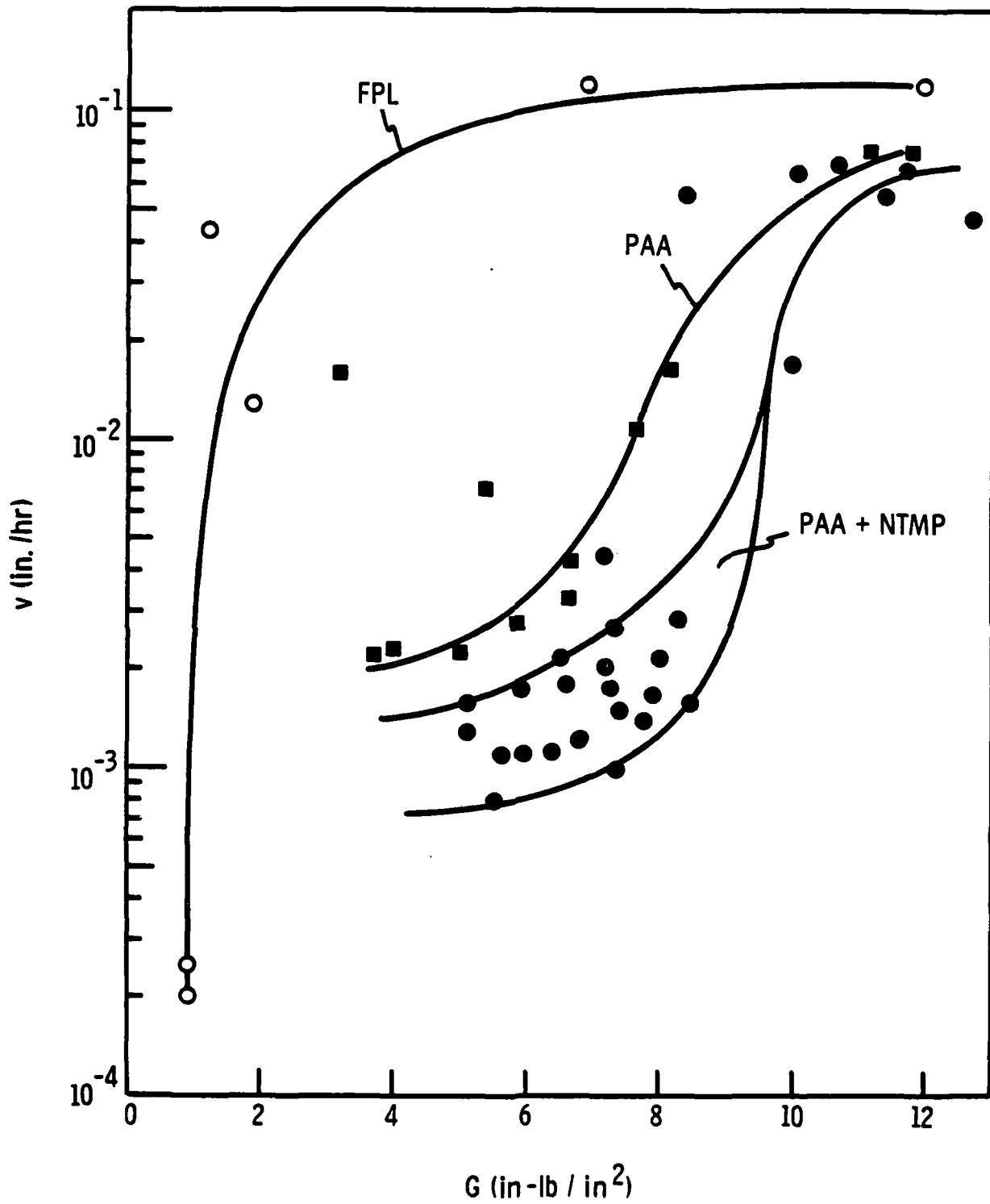


Figure 7. Average crack velocity, v , as a function of G , the fracture energy.

markings on the edge of the adherends that record the position of the crack front with time, was examined visually. In the case of the FPL adherends, the failed surface appeared "dull" or "stained", with heavier stains concentrated close to the initial position of the crack front. In addition, once crack propagation had begun at a particular oxide/adhesive interface, the crack continued to follow along that interface with little or no tendency to transfer through the adhesive to the oxide/adhesive interface on the other side of the adhesive.

On PAA adherends (and to an even greater extent on NTMP-treated PAA adherends), the crack path was not confined exclusively to one oxide/adhesive interface. As was the case with FPL, the regions of initial crack propagation appeared dull or stained, but further along the fracture surface the appearance of the aluminum side of the fracture took on a "shiny" appearance with a slight purple sheen. On the adherends treated in high concentration (200-500 ppm) NTMP solutions, and in 80°C solutions the final increment of crack extension often consisted of regions where crack propagation has occurred wholly within the adhesive layer.

Scanning Microscopy

Scanning electron microscopy (SEM) was used to characterize the fracture surfaces, particularly the aluminum side of these surfaces. SEM confirmed that once a warm, wet environment is established at the crack tip, the crack path always transfers from its initial path in the adhesive to the oxide/adhesive interface, and that initial crack propagation is associated with conversion of the original oxide to boehmite. This transfer always occurred, even on PAA adherends treated in high

concentrations of inhibitor solution; Fig. 8 shows such a surface region on a 100-ppm NTMP-treated PAA adherend.

For PAA adherends (without inhibitor treatment), STEM examination of the fracture surface revealed that the dull regions of the surface corresponded to a hydrated surface, and the shiny regions corresponded to an oxide surface coated with a thin adhesive layer (Fig. 9). This transition from a dull to a shiny surface appearance occurred during the final increment of crack movement. In the lower half of Fig. 9a, the surface, at high magnification, had the cornflake morphology of boehmite (similar to Fig. 8). A higher magnification view of the transition between dull and shiny regions is shown in Fig. 9b. Conversion of the oxide to hydroxide is probably occurring at such a low rate that it is no longer a precursor to crack propagation, and propagation through the adhesive becomes a more favorable mechanism of crack growth. The crack moves progressively away from the interface region until it is wholly within the adhesive layers. The adhesive is deformed by the passage of the crack front until a deformation limit is exceeded, at which point it recoils to form the structures seen in Fig. 9c.

On PAA treated adherends in the presence of the NTMP inhibitor, the transition region, indicating transfer of the crack path away from the oxide/adhesive interface, occurs at a much earlier point in time. Figures 10a and 10b show the fracture path on an adherend treated in a 200-ppm solution of NTMP. The crack has propagated through the adhesive (but is still quite close to the interface as no fibres from the dacron mat are observed). Because moisture was still available to the oxide, with the passage of sufficient time (judged from the position of this

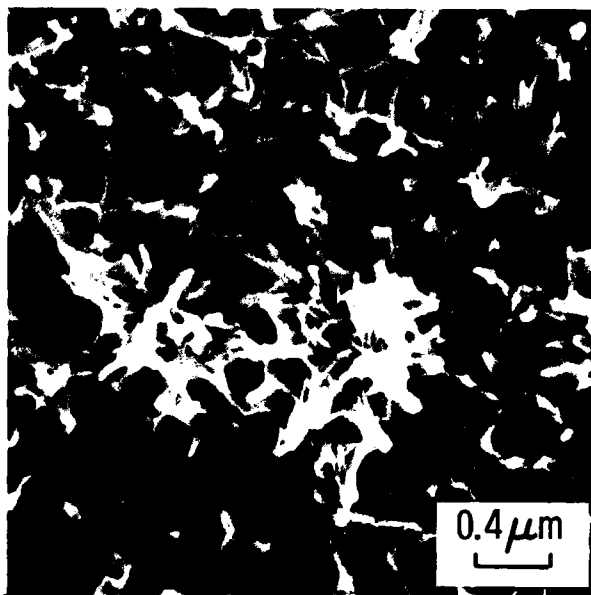


Figure 8. SEM micrograph of "dull" region on Al side of wedge test failure surface. Adherend was PAA-treated in 100-ppm NTMP solution.

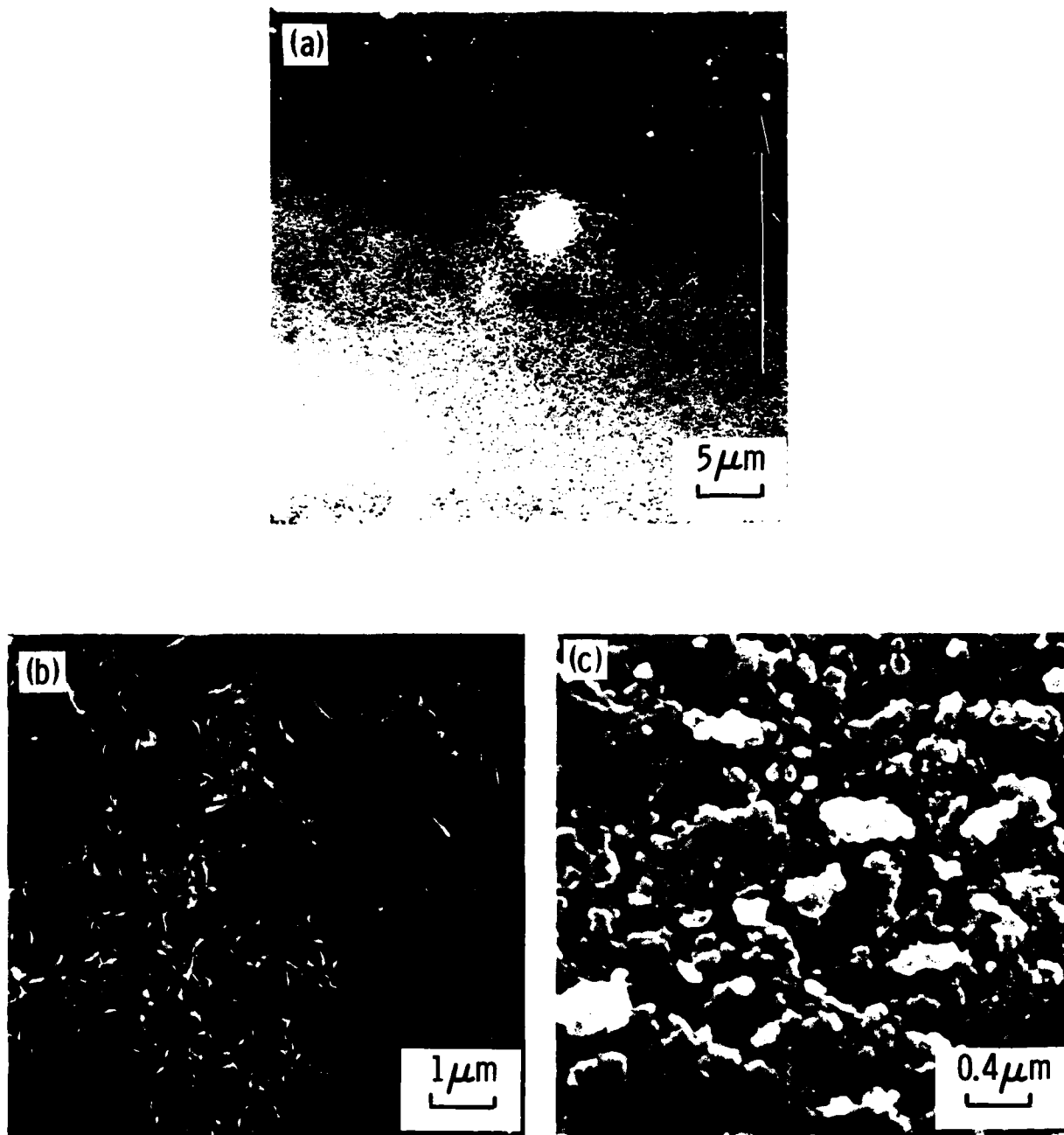
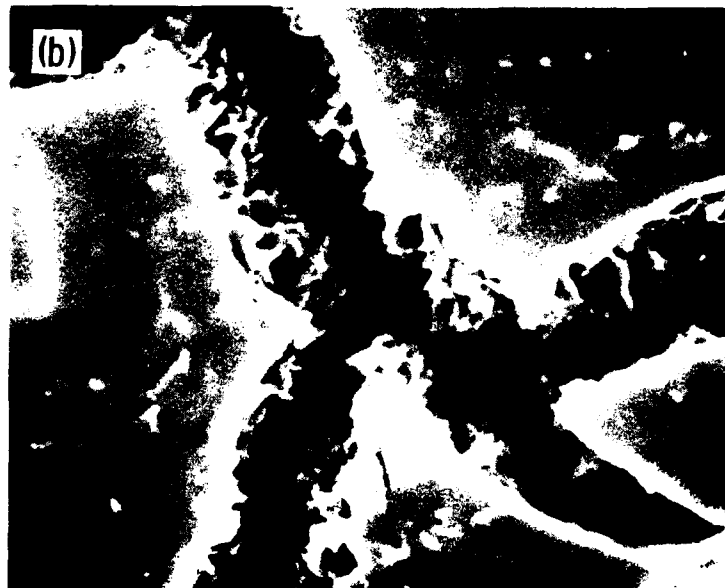


Figure 9. SEM micrographs of: (a) transition region on Al side of PAA wedge-test failure surface (arrow denotes direction of crack propagation); (b) transition region at higher magnification; (c) failure through near-surface adhesive layer.



2 μ m



3.5 μ m

Figure 10. SEM micrographs of Al side of failure surface on PAA adherend treated in 200-ppm NTMP solution showing hydroxide formation after crack propagation through the adhesive layer.

region on the fracture surface to be at least 100 hours), the oxide under the adhesive has transformed to boehmite. In fact, sufficient time has elapsed to allow the formation of bayerite atop the boehmite flakes and it can be seen distorting the adhesive layer in Fig. 10a. The cracks in the adhesive layer seen in Fig. 10 are also a direct result of oxide-to-hydroxide conversion. The formation of boehmite from the initial oxide involves a lattice expansion, and more importantly, the flake morphology adopted by boehmite is considerably more open than that of the amorphous oxide. This results in a ~ 3-fold increase in the thickness of the layer under the adhesive,⁽⁷⁾ and the consequent strain produces cracks in the adhesive. The boehmite structure of the underlying layer is seen very clearly in Fig. 10b.

3.5 SURFACE ANALYSIS OF WEDGE TEST FAILURE SURFACES

Both shiny and dull aluminum-side fracture surfaces from PAA adherends were analyzed by XPS (Table 2). The dull surface was very close in composition to the FPL-failure surface; both surfaces are identical in appearance, being covered with the "cornflake" structure of boehmite. The shiny surface on the other hand, exhibited a very low aluminum concentration and a high carbon concentration. This confirms the SEM evidence that the shiny regions appear to be ruptured adhesive.

TABLE 2

Surface Composition of Al Side Of Wedge
Test Failures As Determined By XPS

Surface Preparation (Appearance)	Composition (%)		
	Al	O	C
FPL	16	52	32
PAA (Dull)	22	46	32
PAA (Shiny)	3	18	79

AES depth profiling confirmed these results; depth profiles obtained for the dull and shiny surfaces are illustrated in Figs. 11 and 12, respectively. The surface of the dull sample comprised a layer $\sim 5,000 \text{ \AA}$ thick of Al-hydroxide. The undulations in the aluminum and oxygen concentrations with depth may be due to density changes in the hydroxide layer but may also result from the sputtering process on the extremely thick hydroxide layer.

The oxide layer on the shiny surface was found to be $\sim 1,000 \text{ \AA}$ thick. Previous work⁽⁸⁾ has shown that the thickness of a typical PAA-oxide, as determined by AES depth profiling, is $\sim 1,000 \text{ \AA}$. Thus the shiny aluminum fracture surface consists of a very thin adhesive layer overlying the original PAA-oxide.

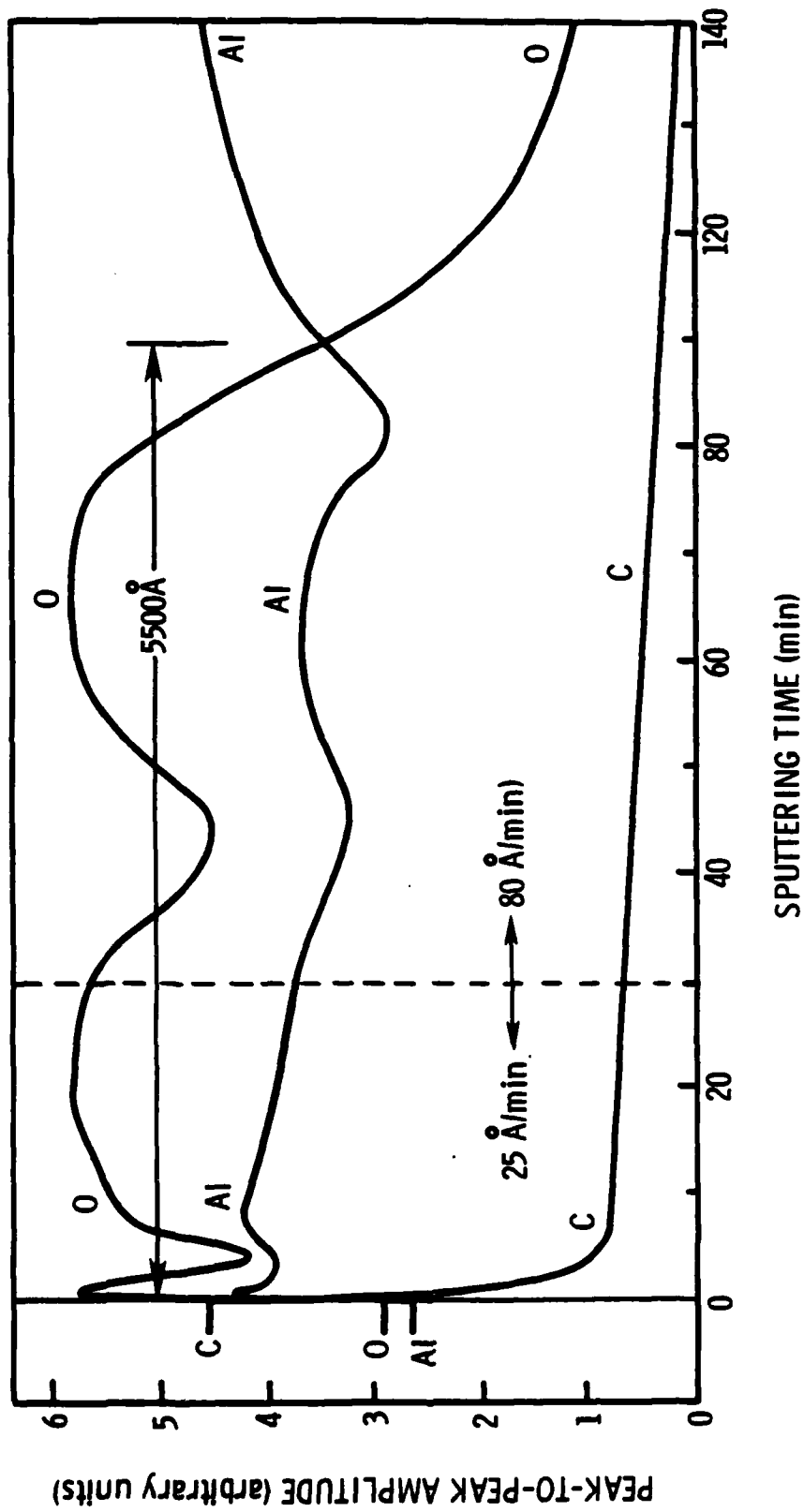


Figure 11. Depth profile of "dull" region on Al side of PAA wedge test failure surface.

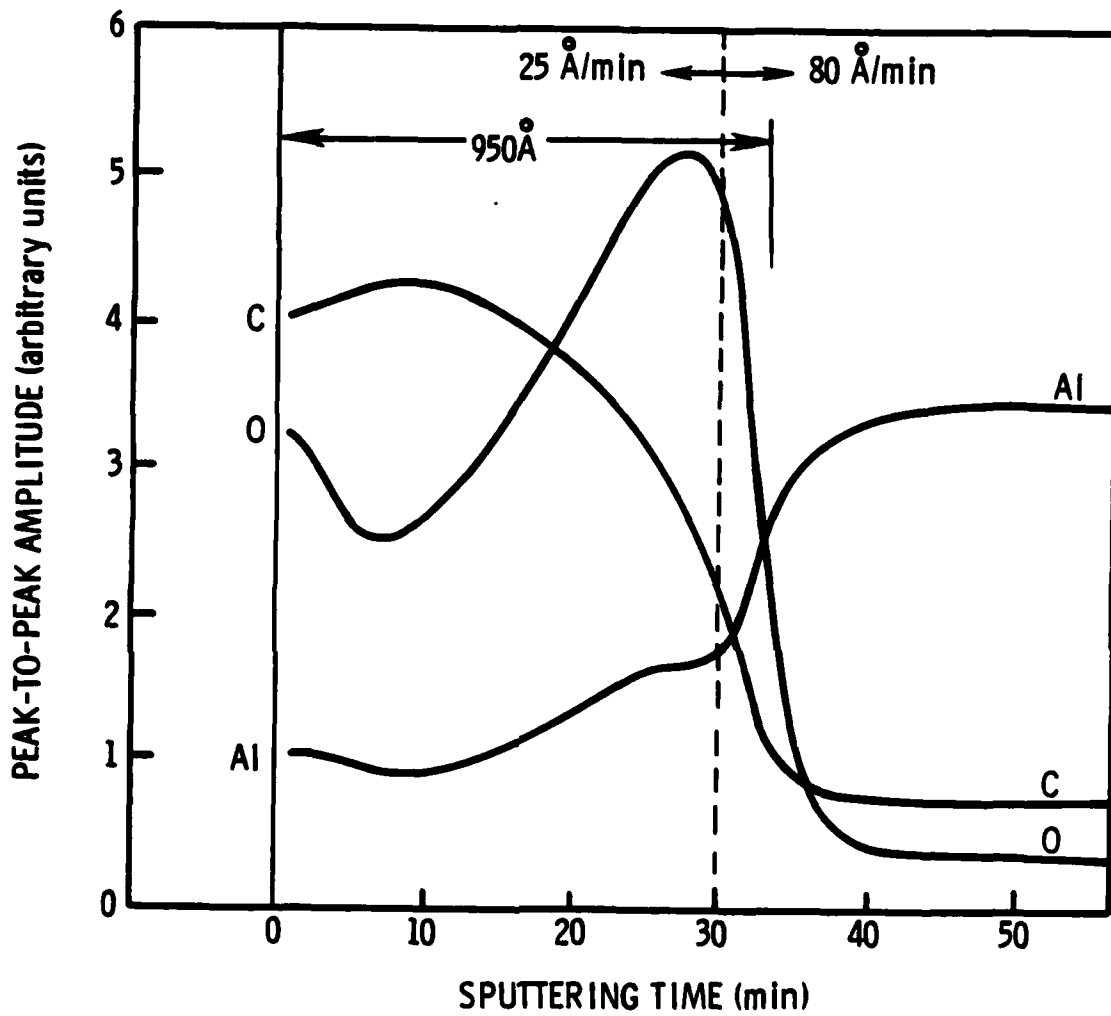


Figure 12. Depth profile of "shiny" region on Al side of PAA wedge test failure surface.

4. DISCUSSION

Inhibitor Adsorption

The range of NTMP solution concentrations used to treat PAA surfaces was identical to that used to treat FPL surfaces. Despite the fact that the P/Al ratio of the PAA-oxide is 0.11 compared with zero for an FPL-oxide, both oxides have a P/Al ratio of ~ 0.2 following treatment in a 300-ppm solution of NTMP at room temperature. This phenomenon is duplicated in the 80°C treatment: at a solution concentration of 300 ppm, the surface coverage for both FPL-and PAA-oxides is in the range 0.4-0.5.

In addition, the surface coverage for FPL-oxide treated in phosphoric acid solution at room temperature saturates at a P/Al of 0.1, i.e., at the same coverage level that occurs on PAA surfaces. This result implies that the surface active sites on the PAA oxide are initially occupied by P-containing groups derived from phosphoric acid. Treatment in room temperature solutions of NTMP results in the adsorption of NTMP groups onto this pre-existing surface or the replacement of at least some of the initial P-containing groups with NTMP. Both of these processes would increase the surface coverage, as measured by the P/Al ratio, but our present experimental results do not allow us to distinguish between these two alternatives. The high surface coverage obtained on FPL surfaces treated in NTMP solutions at 80°C is most likely related to multilayer surface coverages⁽³⁾ and this is probably also true for PAA surfaces treated in a similar fashion.

Initial Bond Strength

The influence of NTMP on initial bond strength was evaluated using the T-peel test. For each of the epoxy-based adhesives used, failure in the T-peel test was cohesive through the adhesive, so that the T-peel strength values were not influenced by the presence of NTMP at the oxide/adhesive interface. These results indicate that the strength of the interface, with or without NTMP, was greater than the peel strength of the strongest epoxy adhesive used, i.e., 50 lb/in.

Some preliminary T-peel tests were conducted using a non-epoxy, structural adhesive/primer combination (nitrile-phenolic). When monolayer NTMP coverage was present on the FPL surface prior to bonding, the T-peels failed close to the polymer/oxide interface. Preliminary analyses of the failed surfaces seemed to indicate that the NTMP had interfered with normal curing processes.

Thus the value of the initial bond strength may be strongly influenced by the degree of compatibility between NTMP and the particular primer and/or adhesive used. We can conclude that NTMP is compatible with epoxy-based systems, but that it appears to interfere with the curing of nitrile-phenolics. Obviously, more information is needed to assess the compatibility of NTMP with other structural adhesive systems currently available.

Bond Durability

The wedge test results clearly demonstrate that the superior bond durability of PAA-treated adherends can be further improved by pretreatment in NTMP inhibitor solution. This is expected as our previous work⁽⁶⁾ had shown that PAA oxides were subject to oxide-to-hydroxide conversion although the reaction rate was slower than that observed for FPL oxides.

Since our previous work^(2,3) had established that long term bond durability is intimately related to the stability of an oxide surface in the presence of moisture, any further increase in oxide stability should result in improvements in bond performance.

Maximum improvements in the bond durability of PAA adherends occurred when a monolayer of the NTMP inhibitor was present on the surface; multilayer coverages, obtained with elevated temperature (80°C) treatment solutions, did not further improve bond durability. Similar results were obtained when FPL adherends were treated in 80°C solutions of NTMP.⁽³⁾ When FPL adherends were treated in a 10-ppm NTMP solution at 80°C, there was a 1.65X increase in surface coverage above that achieved through RT treatment. Use of XPS to study wedge-test failure surfaces with these high surface coverage levels revealed that P was present on both sides of the failure, implying that the crack path had been through the multilayer surface film produced by the elevated temperature treatment.⁽³⁾ Surface coverage data was not taken for 80°C treatment of PAA in 10 ppm NTMP solutions, but treatment of PAA in an 80°C, 300-ppm NTMP solution did give a 1.45X increase in surface coverage over the level recorded for a similar treatment at room temperature. Thus, a similar mechanism may be operative when PAA adherends have multiple layers of NTMP between the oxide and the adhesive; failure can occur through the NTMP layers so that although there is an improvement in bond durability over that of untreated PAA adherends, this improvement may not be as good as that achieved when a monolayer of NTMP is present.

Discussion of the wedge test results is greatly facilitated by the fracture mechanics approach which was used in the preparation of Figure 7.

Initial crack lengths prior to exposure to the humid environment (i.e., the crack length at 1 hour plotted in Figs. 3-6) were similar for all adherends, and thus the initial G values are similar for all adherends. This initial crack extension force gave rise to similar initial crack velocities, regardless of whether the adherend surface preparation included treatment with the inhibitor NTMP.

More information must be assembled before definitive statements can be made regarding the initial stages of crack growth during the wedge test, but some preliminary conclusions can be inferred through reference to work by Patrick et al.⁽⁹⁾ They used tapered DCB specimens of adhesively-bonded 2024 Al containing an initial precrack at the center of the bond line and established that when a static load (well below that needed to cause unstable cracking) was applied in the presence of either liquid water or 96% RH air, cracking occurred at the adhesive/adherend interface and was not a continuation of the initial precrack. The interfacial failure was initiated just below or slightly behind the crack tip of the precrack, i.e., in the region of interaction of the stress field, due to the crack tip, and the adherend surfaces.

Examination of the fracture surfaces indicate that a similar re-initiation step may be occurring in the initial stages of our wedge tests. On FPL-prepared adherends in particular, there is an abrupt transition from cohesive to adhesive failure during the first hour of exposure to the humid environment. This transition is less abrupt for the PAA adherends and on PAA treated with 300-ppm NTMP; there is effectively an "incubation period" before interfacial failure is seen. Future experimental procedures should include more careful attention to processes

occurring in the initial stages of crack growth, particularly for adherends treated in NTMP. Based on our results, we must tentatively conclude that the re-initiation of the crack in the presence of moisture occurs by hydration of the original oxide to give boehmite, but this conclusion must be verified experimentally.

Regardless of the exact mechanism, once interfacial cracking has begun on FPL adherends (without inhibitor treatment), the initial crack velocity is maintained to very low values of G . (It should be kept in mind that G is not a simple function of time but is related to crack length.) The fact that the rate of crack growth is relatively constant over a wide range of G values indicates that the mechanism of crack growth is independent of the driving force. The conversion of oxide to hydroxide is such a stress independent mechanism, and STEM examination of fracture surfaces had previously led to its identification as the mechanism by which adhesive bonds fail in the presence of moisture.(2)

As seen in Fig. 7, the behavior of the PAA adherends is quite different. At levels of G which are still relatively high, the crack velocity began to fall, and it then leveled off two orders of magnitude below its initial value. SEM examination of these fracture surfaces (Section 3.4) has shown that over the course of the wedge test the locus of failure initially transfers from oxide/adhesive interface, and in the latter stages to the adhesive near the interface. For the PAA adherends treated in higher-concentration NTMP solutions, this transfer occurs quite early in the test and, in the latter stages, the cracking occurs through the adhesive. Thus, the decrease in crack velocity is probably due to the occurrence of this transition, and the crack growth rate at

the lower level plateau may be characteristic of the adhesive. More testing is currently in progress to verify these conclusions.

In summary, the hydration inhibitor NTMP can be used to improve the bond durability of adherends prepared by the PAA process. Maximum improvement in bond durability is obtained with monolayer coverages of NTMP. When epoxy-based adhesive systems are used, the presence of NTMP at the oxide-adhesive interface does not degrade the initial bond strength.

5. REFERENCES

1. J.D. Venables, D.K. McNamara, J.M. Chen, T.S. Sun, and R.L. Hopping: "Oxide morphologies on aluminum prepared for adhesive bonding", Appl. Surf. Sci., Vol. 3, pp. 88-98 (1979).
2. J.D. Venables, D.K. McNamara, J.M. Chen, B.M. Ditchek, T.I. Morgenthaler, and T.S. Sun: "Effect of moisture on adhesively bonded aluminum structures", Proc. 12th Nat. SAMPE Tech. Conf., Seattle, WA. (1980).
3. J.S. Ahearn, G.D. Davis, A. Desai, and J.D. Venables: "Mechanical properties of adhesively bonded aluminum structures protected with hydration inhibitors", Martin Marietta Laboratories, Tech. Report TR 81-46c (October, 1981).
4. D. Broek, "Elementary Engineering Fracture Mechanics", Sijthoff and Noordhoff, The Netherlands, p. 154 (1978).
5. M.H. Stone and T. Peet: "Evaluation of the wedge cleavage test for assessment of durability of adhesive bonded joints", Royal Aircraft Establishment Tech. Memo MAT 349, (July, 1980).
6. G.D. Davis, T.S. Sun, J.S. Ahearn, and J.D. Venables: "Application of surface behaviour diagrams to the study of hydration of phosphoric acid-anodized aluminum", J. Mater. Sci., Vol. 17, pp. 1807-1818 (1982).
7. W. Vedder and D.A. Vermilyea: "Aluminum + Water Reaction", Trans. Faraday Soc., 65, 561 (1969).
8. T.S. Sun, D.K. McNamara, J.S. Ahearn, J.M. Chen, B. Ditchek, and J.D. Venables: "Interpretation of AES depth profiles of porous Al anodic oxide", Appl. Surf. Sci., Vol. 5, pp. 406-425 (1980).
9. R.L. Patrick, J.A. Brown, L.E. Verhoeven, E.J. Ripling, and S. Mostovoy: "Stress-solvolytic failure of an adhesive bond", J. Adhes., Vol. 1, pp. 136-141 (1969).

2-8

DT